Advances in Science and Technology Research Journal

Advances in Science and Technology Research Journal, 2025, 19(9), 504–515
https://doi.org/10.12913/22998624/207677
ISSN 2299-8624, License CC-BY 4.0

Received: 2025.05.21
Accepted: 2025.07.15
Published: 2025.08.01

Numerical and experimental analysis of thermoplastic deformation in pure titanium using the Anand model for biomedical implant design

Jakub Bańczerowski[1], Marek Pawlikowski[1]

[1] Faculty of Mechanical and Industrial Engineering, Warsaw University of Technology, Narbutta 85, 02-524 Warsaw, Poland
* Corresponding author's e-mail: jakub.banczerowski@pw.edu.pl

ABSTRACT

This study used the Anand constitutive model to predict how commercially pure Grade 2 titanium behaves during thermoplastic deformation, with the goal of making it more suitable for load-bearing medical implants. Although titanium alloys like Ti6Al4V are commonly used in implants, there are concerns about the release of toxic ions, which encourages the search for safer options like pure titanium. To strengthen pure titanium, this research focused on thermo-mechanical processing (TMP). The study combined experimental compression tests (conducted at 400–600 °C and strain rates of 0.01–1.0 s^{-1}) with computer simulations based on the Anand model. The model can describe important material behaviours, such as strain hardening, dynamic recovery, as well as sensitivity to temperature and strain rate. Originally developed for soft metals, the Anand model was successfully adapted to pure titanium and showed high accuracy in predicting material behaviour at elevated temperatures and moderate strain rates. Some prediction errors at 400 °C were likely due to incomplete dynamic recrystallisation. The best fit of the studied model to the experimental results was achieved for the temperature 600 °C and strain rate 0.01 s^{-1} with adjusted R-square equal 0.988 and root mean square error equal 3.941. The model was further tested under specific conditions (450 °C, 550 °C, strain rate of 0.5 s^{-1}) and achieved flow stress prediction errors below 8%. In summary, this work provides a reliable and efficient tool for optimising TMP processes, reducing the need for costly trial-and-error methods, and supporting the production of patient-specific implants made from pure titanium.

Keywords: Anand model, thermoplastic deformation, pure titanium, model validation, FEM.

INTRODUCTION

Degenerative diseases of the hip and knee joints affect millions globally, driving the demand for improved arthroplasty procedures and long-lasting orthopaedic implants that combine biocompatibility with bone-like mechanical properties [1, 2]. Titanium alloys, such as Ti6Al4V are widely used in implant manufacturing due to their high strength [3]. However, clinical studies have raised concerns over ion release – vanadium ions exhibit cytotoxic effects at concentrations as low as 1 μM, while aluminium accumulation is associated with neurological disorders [4–6].

In contrast, commercially pure titanium avoids these toxicological risks and offers excellent biocompatibility. However, its relatively low yield strength (170–480 MPa) significantly limits its use in load-bearing applications, which typically demand strengths in the range of 800–1000 MPa. As a result, pure titanium is mainly used in non-load-bearing applications, such as dental implants. Recent advances in thermomechanical

processing (TMP) offer possibilities to enhance the mechanical strength of commercially pure titanium through controlled plastic deformation. However, the complex relations of titanium strain hardening and dynamic recovery mechanisms at elevated temperatures (400–600 °C) results in highly nonlinear stress–strain behaviour. This complexity makes process optimisation difficult, with current approaches relying heavily on trial-and-error experimentation, resulting in significant time and resource costs.

This study addresses these challenges by proposing a thermomechanical processing for commercially pure titanium at intermediate temperatures, with the aim of achieving the yield strengths suitable for orthopaedic load-bearing implants. A numerical model was proposed to simulate the plastic deformation process, enabling precise parameter identification, optimisation, and prediction of the resulting mechanical properties, reducing trail-and-error experimental workload.

The Anand viscoplastic constitutive model was adopted to simulate the thermoplastic deformation of commercially pure titanium at intermediate temperatures. Although originally developed for soft metals and solders, the Anand model was adapted here to account for the strain-rate sensitivity, temperature-dependent behaviour, and work hardening of titanium [7, 8]. By integrating experimental data from compression tests with finite element simulations, the model is calibrated and validated for pure titanium. This approach makes it possible to predict material behaviour with high accuracy and significantly reduce the need for experimental iterations.

The implementation extends Anand's original model by integrating temperature-dependent Young's modulus and experimentally determined friction boundary conditions. The model is validated against compression test data, demonstrating fair prediction accuracy at 400–600 °C. It also allows prediction of the elastic–plastic transition, though with limited precision.

The proposed numerical framework offers a practical and efficient approach to process planning and optimisation, enabling the precise adjustment of deformation parameters. This supports the manufacturing of titanium implants with custom-tailored mechanical properties, ensuring both improved performance and long-term reliability in biomedical applications.

METHODS

Mathematical model

Accurate simulation and optimisation of thermomechanical processes rely on a thorough understanding of the technological characteristics of the material. For each processing method, specific material properties determine its suitability. In plastic deformation processes, the key property is the yield stress (σ), defined as the stress required to initiate and sustain plastic flow under uniaxial loading. Yield stress is influenced by strain (ε), strain rate ($\dot{\varepsilon}$), temperature (T), as well as prior deformation history [9]. To capture the complex, temperature-dependent behaviour of materials during plastic deformation, this study adopted the Anand viscoplastic model, originally formulated by Anand and Brown for high-temperature metal deformation [10]. The model describes isotropic elastic-viscoplastic behaviour without explicitly separating yield criteria and hardening rules [11, 12]. While traditionally applied to soft solders and alloys [13–17], here it is adapted for commercially pure titanium, which exhibits significant strain hardening and dynamic recovery during thermomechanical processing. In this paper, strengthening mechanisms such as changes in dislocation density and grain/subgrain structure are considered to be characterised by a deformation resistance variable s, which is related to the stress σ by:

$$\sigma = cs; c < 1 \tag{1}$$

where: c is a function of strain rate and temperature, defined as.

$$c = \frac{1}{\xi}\sinh^{-1}\left\{\left[\frac{\dot{\varepsilon_p}}{A}\exp\left(\frac{Q}{RT}\right)\right]^m\right\} \tag{2}$$

where: ξ is a dimensionless scaling factor, $\dot{\varepsilon_p}$ is the plastic strain rate, A is material constant, Q is the activation energy, R is the gas constant, T is the absolute temperature and m is the strain-rate sensitivity.

The Anand flow equation relates plastic strain rate to stress and deformation resistance:

$$\dot{\varepsilon_p} = A\exp\left(-\frac{Q}{RT}\right)\left[\sinh\left(\xi\frac{\sigma}{s}\right)\right]^{\frac{1}{m}} \tag{3}$$

The evolution of deformation resistance is governed by:

$$\dot{s} = h(\sigma, s, T)\dot{\varepsilon_p} \tag{4}$$

where: h accounts for strain hardening and dynamic recovery. A common formulation of h is:

$$\dot{s} = \left[h_0 \left(A - \frac{s}{s^*}\right)^a \operatorname{sign}\left(1 - \frac{s}{s^*}\right)\right] \dot{\varepsilon_p};\ a > 1 \quad (5)$$

where: s^* is the saturation deformation resistance at a given strain rate and temperature, h_0 is the hardening/softening coefficient, and a controls the rate of saturation. Analogously to Equation 1, the saturation stress is defined as:

$$\sigma^* = cs^* \quad (6)$$

Combining Equations 2 and 5, the saturation stress can be expressed as:

$$\sigma^* = \frac{\hat{s}}{\xi}\left[\frac{\dot{\varepsilon_p}}{A}\exp\frac{Q}{RT}\right]^n \sinh^{-1}\left\{\left[\frac{\dot{\varepsilon_p}}{A}\exp\frac{Q}{RT}\right]^m\right\} \quad (7)$$

where: m is the strain rate sensitivity n is the strain rate sensitivity for the saturation value, and $\hat{s}$ is coefficient of deformation resistance.

Finally, Equations 1 and 4 lead to equation for differentiating stress with respect to plastic strain yields:

$$\frac{d\sigma}{d\varepsilon_p} = ch_0 \left|1 - \frac{\sigma}{\sigma^*}\right| \operatorname{sign}\left(1 - \frac{\sigma}{\sigma^*}\right);\ a > 1 \quad (8)$$

Integrating Equation 8, the stress evolution during plastic deformation is given by:

$$\sigma = \sigma^* - \left[\begin{matrix}(\sigma^* - cs_0)^{1-a} + \\ + (a+1)\{(ch_0)(\sigma^*)^{-a}\}\varepsilon_p\end{matrix}\right]^{1/(1-a)} \quad (9)$$

where: s_0 is the initial value of the deformation resistance s.

Experimental procedure

Determining plasticity under hot-working conditions is challenging, as the structure of the material is influenced by plastic deformation, hardening mechanisms, and thermally activated, time-dependent phenomena that can lead to material weakening [18, 19]. To characterise these effects, an experiment was conducted to gather data on the response of the material under varying temperature conditions and strain rates, following standard procedures used by numerous researchers [20–26].

Uniaxial compression tests were performed on commercially pure Grade 2 titanium to characterise its thermoplastic response under conditions representative of industrial forming processes. Cylindrical specimens (⌀10×12 mm) were machined from hot-rolled bars, with the longitudinal axis aligned parallel to the rolling direction to maintain microstructural consistency. Tests were conducted across three temperatures (400, 500, 600 °C) and three strain rates (0.01, 0.1, 1 s^{-1}), covering the typical hot-working range for titanium-based orthopaedic components. Details of the full experimental procedure are available in the authors' previous work [27]. Figure 1a presents the pure titanium samples, while Figure 1b shows the experimental setup. The experimental stress–strain curves were used as input for a four-stage parameter identification protocol implemented in MATLAB, employing a nonlinear least squares method. This procedure follows the protocol outlined in [7], with only the key steps summarised here:

1) saturation stress is extracted from the stress–strain curves at constant temperatures and strain rates.
2) parameters A, Q, ξ, m, $\hat{s}$ and n (Equation 7) are computed via nonlinear least squares, treating $\hat{s}/\xi$ as single parameter. Constants are computed based on experimental parameters, i.e. deformation rate and maximal stress.
3) $\hat{s}$ and ξ are derived from the previous step, with ξ adjusted to keep c (Equation 2) around unity. $\hat{s}$ is then determined from $\hat{s}/\xi$.
4) constants ch_0, cs_0, a (Equation 8) are calculated using nonlinear least squares from constant strain rate data.

With c known, h_0 and s_0 are then obtained. The curve-fitting process was supported by a literature review to ensure the constants remained within reasonable physical limits [12, 13, 15, 17, 28]. In addition, the four-stage parameter calibration has been successfully used in similar studies [12] and [14], providing consistent results as well as allowing good predictive capability within and beyond the calibrated range.

Numerical model and implementation

The objective of the numerical analysis was to verify the accuracy of the Anand model implementation by comparing simulation results with the experimental data from uniaxial compression tests. To ensure fidelity, the simulations closely replicated the conditions of the physical experiments. Simulations were conducted in ANSYS Workbench 2020R2. Separate projects were created for each temperature level (400–600 °C), with subcases defined by strain rate. The Anand viscoplastic model was implemented using the

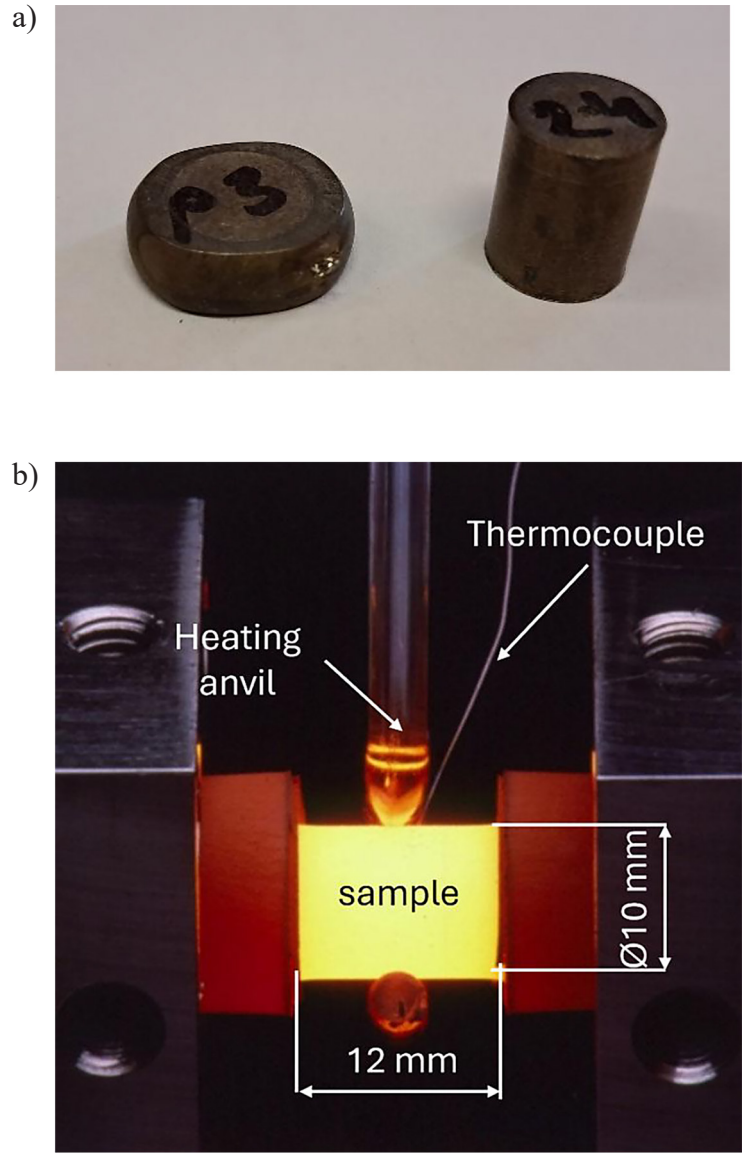

Figure 1. (a) Samples before (right) and after (left) TMP, (b) setup of a Gleeble TMP experiment. Heated cylindrical sample (⌀10 × 12) just before compression

previously identified material parameters. The geometry consisted of a cylindrical specimen (⌀10 × 12 mm) compressed between two rigid anvils (25 × 25 × 5 mm), which were modelled as non-deformable bodies (Figure 2). Material properties were defined in the Engineering Data section, including the temperature-dependent Young's modulus. While the room temperature modulus was set at 110 GPa [29], values at elevated temperatures were extrapolated from experimental stress-strain data (Figure 3 and Table 1) [30]. To mimic the industrial hot-working conditions, contact between the sample and anvils was set as frictional with a coefficient of 0.05, simulating graphite lubrication. A hexahedral mesh was used (Figure 2c), with 1 mm elements generating 3874 elements and 18357 nodes. Mesh sensitivity analysis confirmed that further refinement yielded negligible accuracy gains but significantly increased computation time. Compression was simulated by displacing the upper anvil downward by 7 mm over a time interval corresponding to the target strain rate. Each simulation was divided into 10 time steps to capture material response evolution. The sample temperature was defined as uniform for each case.

A total of 25 simulations were performed, covering all combinations of temperature and strain rate. Each case was solved using the PCG (Preconditioned Conjugate Gradient) solver,

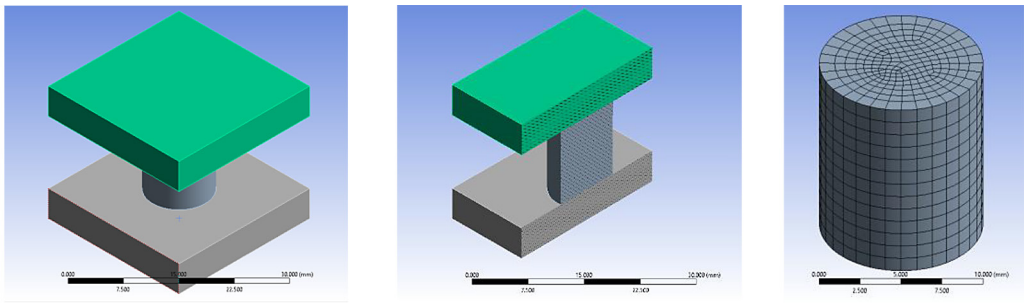

a) b) c)

Figure 2. Geometric model used in the simulation: full assembly view (a), cross-sectional view (b), and meshed sample (c)

Table 1. Young's modulus of Grade 2 titanium as a function of temperature [30]

Temperature [C]	Young's modulus [MPa]	Poisson's ratio	Bulk modulus [Pa]	Shear modulus [Pa]
20	1.1e+05	0.37	1.41e+11	4.01e+10
400	8450	0.37	1.08e+10	3.08e+09
500	5580	0.37	7.15e+09	2.04e+09
600	4500	0.37	5.77e+09	1.64e+09

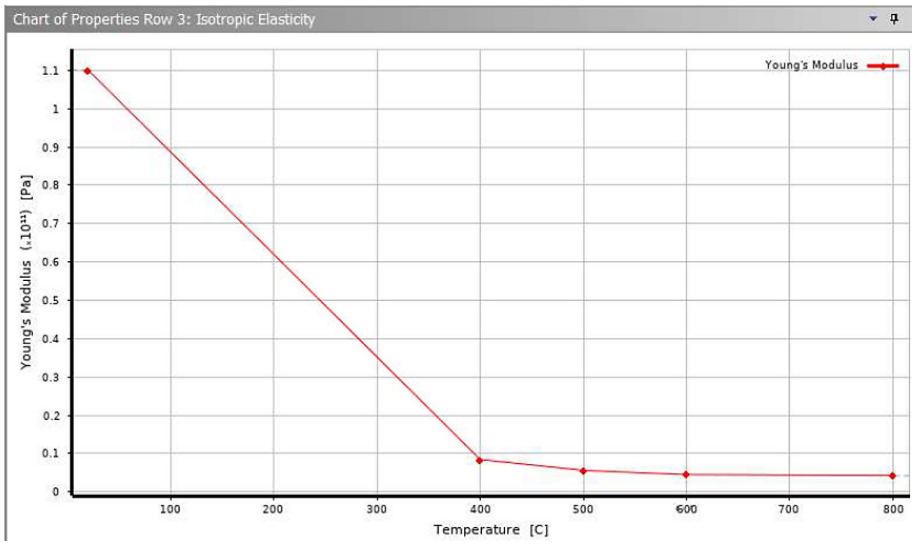

Figure 3. Young's modulus of Grade 2 titanium as a function of temperature [30]

which proved effective for handling large, nonlinear deformations. Computation times ranged from 5 to 15 minutes per simulation.

RESULTS

Experimental results

For the purpose of developing and validating the constitutive model, selected results at 400 °C and 600 °C were used, as presented in Figures 4a and 4b, respectively. At higher strain rates at lower temperature, the curves take on an irregular shape. Such a curve profile indicates the so-called Portevin–Le Chatelier effect, which commonly occurs in metals, although the mechanisms behind its formation vary [31, 32]. For commercially pure α-titanium, an explanation of this behaviour was provided by Prasad [33]. During deformation, mobile dislocations are halted by interstitial elements such as C and N. Then, after overcoming these obstacles, the dislocation rapidly jumps to the next barrier, which results in the effect visible on the curve.

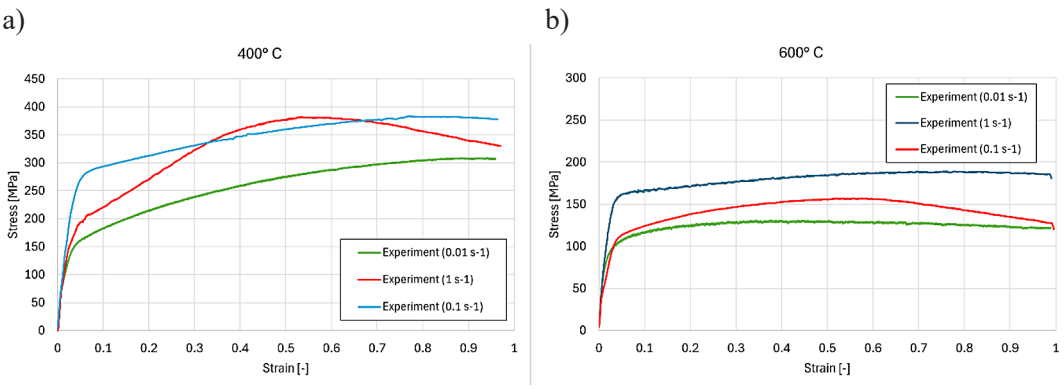

Figure 4. True stress–strain curves obtained from uniaxial compression tests of Grade 2 titanium at (a) 400 °C and (b) 600 °C for various strain rates (0.01–1 s^{-1}), used for constitutive model calibration and validation

The nature of the curves changes slightly for tests conducted at higher temperatures. The curves transition directly from Phase I (strain hardening) to Phase II – plastic flow. Similar behaviour was observed by Nemat-Nasser and Zeng [18, 34]. In the case of lower strain rates, the curve shows a slight decline, indicating thermal softening (Figure 4).

Identification of model parameters

The parameters a, h_0 and s_0 of the mathematical model (9) were identified based on the experimental results using curve fitting method, in particular nonlinear least square method which is widely accepted by scientific community as a reliable tool for the desired tasks. The authors decided that the chosen method provides a reliable and computationally efficient solution fully consistent with the goals of the study and comparable with approaches used in related research. Additionally, nonlinear least square method is implemented in widely used mathematical tools like MATLAB or Wolfram Mathematica, which allows for quick implementation of this method for desired calculations. The parameter values are presented in Table 2 where the calculated constants of the model are also shown. The fitted curves were compared to the experimental data in order to assess the correctness of the fit (Figure 5). The nonlinear least square method was used to fit model for the 0.01 s^{-1} and 1 s^{-1} strain rates simultaneously. Thus, one set of the parameters enabling to model the material behaviour in a wide deformation rate range was obtained. The middle curves (for 0.1 s^{-1}) represent a verification of the parameter identification. They are obtained by introducing the calibrated parameters into (9). The model fits the experimental data well in most cases. It is worth noting that the model reflects both the initial phase of elastic deformation and the plastic phase of TMP processing. To evaluate the model fit, both visual comparison and statistical regression metrics

Table 2. Identified parameters for the Anand model, obtained through nonlinear least squares fitting to experimental stress–strain data for the strain rate span 0.01÷1 s^{-1} and calculated model constants

Temp [°C]	400	600	Temp [°C]	400	600
0.01 s^{-1}			1 s^{-1}		
Q [J/mol]	382444	300000	Q [J/mol]	382444	300000
s_0 [MPa]	46.05	2.6	s_0 [MPa]	46.05	2.6
A	2.33E+06	1.49E+05	A	2.33E+06	1.49E+05
ξ	50	29	ξ	50	29
m	0.846	0.973	m	0.846	0.973
h_0	3605.8	13156.7	h_0	3605.8	13156.7
$\hat{S}$	74.6	44.69	$\hat{S}$	74.6	44.69
n	0.034	0.060	n	0.034	0.060
a	1.176	1.76	a	1.176	1.76
$\hat{S}/\xi$	1.492	1.541	$\hat{S}/\xi$	1.492	1.541
c	0.844	1.036	c	0.922	1.190

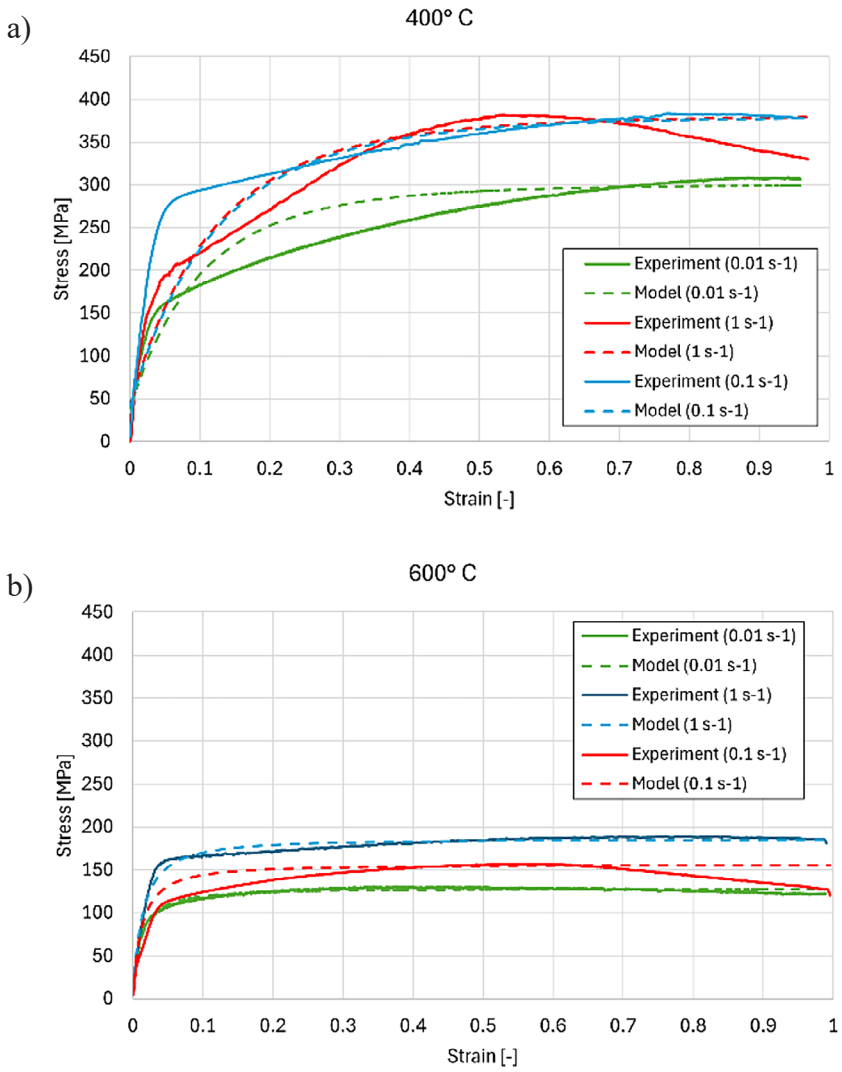

Figure 5. Curve fitting effects for (a) 400 °C set, (b) 600 °C. Experimental results are presented with continuous lines and fitted curves are visible as dashed lines

were used: sum of squared errors (SSE), R-squared, adjusted R-squared, and root mean square error (RMSE) between experimental and predicted values [35–37]. The results, summarised in Table 3, indicate strong agreement. High R-squared values and low RMSE and SSE confirm a good fit overall. As expected, the model performed least accurately at 400 °C and a strain rate of 1 s^{-1} where fitting proved only partially successful.

Model validation through numerical analyses

To validate the predictive capability of the developed numerical model, simulations were conducted for the processing conditions not previously tested experimentally. Specifically, the model was used to predict the material response at 450 °C and 550 °C with a strain rate of 0.1 s^{-1}, 0.5 s^{-1} and 1 s^{-1}. The corresponding stress-strain curves were generated numerically. Subsequently, physical compression tests were carried out under identical conditions to compare the experimental results with the model predictions. Additionally, the experiments for the 400 °C and 500 °C were conducted at the rate 0,5 s^{-1}.In all cases the numerical calculations values are comparatively similar with experimental results. The slope of the experimental stress-strain curves follows the slope of the experiment, especially in the plastic region. Unfortunately, due to phenomena taking place during the thermal processing (most likely due to dynamic recrystallisation) the stress in the experimental curve drops. The presented model is unable to follow this effect (Figure 6 a, b).

Table 3. Anand model parameters and statistical fit metrics for commercially pure titanium

Temp.	400 °C		
$\dot{\varepsilon}$ [1 s^{-1}]	0.01	0.1	1
SSE	4525	1.21E+04	2.44E+04
R-square	0.9887	0.975	0.9582
Adjusted R-squared	0.9881	0.9737	0.9558
RMSE	9.07	14.86	21.87
Temp.	600 °C		
$\dot{\varepsilon}$ [1 s^{-1}]	0.01	0.1	1
SSE	1582	3211	1819
R-squared	0.9884	0.9698	0.9815
Adjusted R-squared	0.988	0.9681	0.9808
RMSE	3.941	7.641	6.157

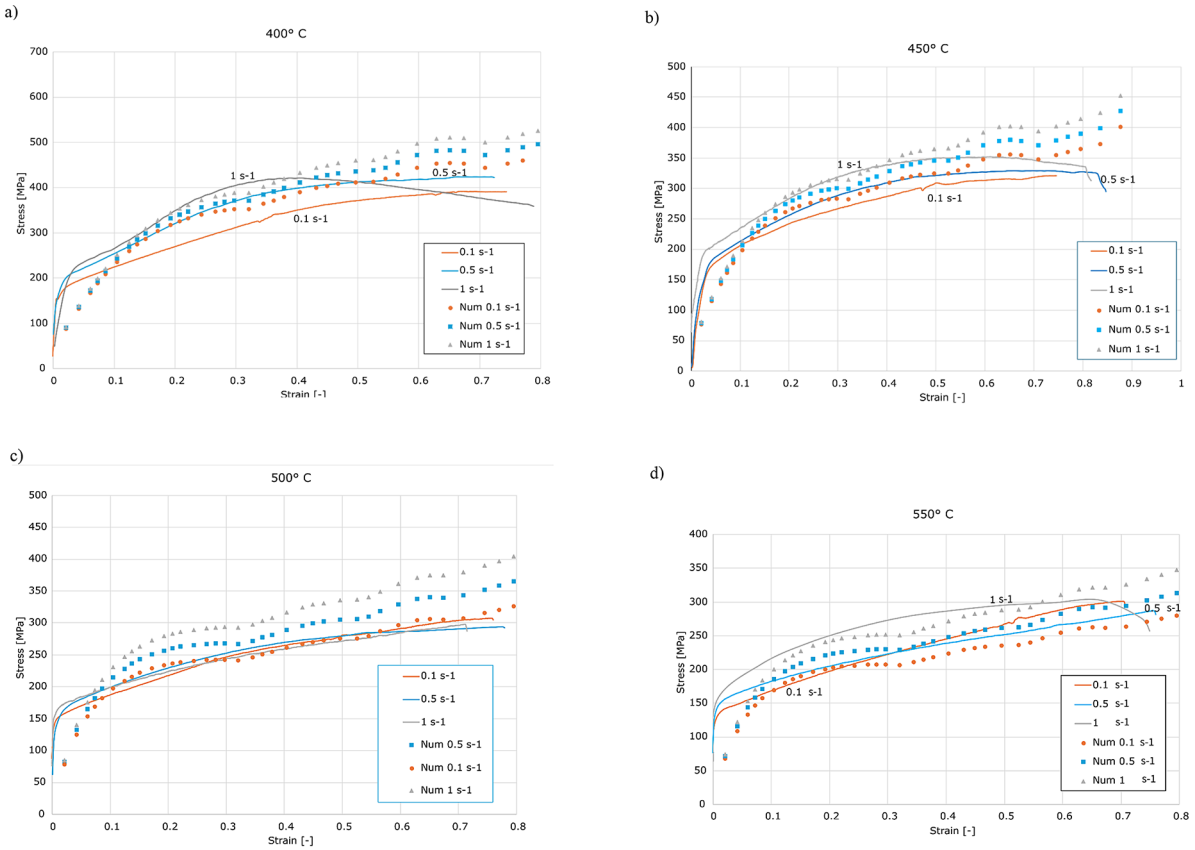

Figure 6. Comparison of FEM simulation results and experimental curves at (a) temperature of 400 °C, (b) temperature 450 °C, (c) temperature 500 °C, (d) temperature 550 °C

DISCUSSION

The implemented Anand model demonstrated a high degree of efficiency in predicting the thermoplastic deformation behaviour of commercially pure titanium across a wide range of processing conditions. Quantitatively, the model achieved excellent agreement with experimental data, as evidenced by high R-squared values (≥ 0.95 in most cases) and low RMSE values, particularly at elevated temperatures where thermally activated mechanisms dominate plastic flow. However, the model exhibits clear limitations in capturing the softening behaviour related to dynamic recrystallisation, as evidenced by stress drops in the experimental curves at lower temperatures (Figure 6a

and 6b). This limitation is inherent to the Anand model, which does not include recrystallisation kinetics or flow softening terms in its original formulation [13]. As a result, the model maintains a strain-hardening response, even in conditions where dynamic recrystallisation leads to stress reduction. Nevertheless, the model performs consistently well across higher temperatures and different strain rates, and it also demonstrates good predictive capability when extrapolated to untested conditions. The issue at 400 °C highlights a local limitation rather than a fundamental flaw in the model, meaning it remains reliable for process optimisation and implant design within the broader temperature range relevant to biomedical applications.

In Anand's original work, the model was applied to lithium [15], yielding parameter values largely consistent with those obtained in the present study, with the exception of $A = 4.25 \times 10^4$ and $h_0 = 1_0$. Cheng et al. [12], studying solder materials, reported a set of constants comparable in magnitude to those for commercially pure titanium, except for a significantly different activation energy Q. Similarly, in the studies on sintered nanosilver [28] and SAC305 solder [26], most parameters aligned closely, with notable deviations again observed in A and Q/R.

Its computational performance was also noteworthy: each full simulation completed within 5–15 minutes using standard PCG solvers in ANSYS, making it suitable for iterative design workflows and real-time parameter optimisation. Importantly, the model retained its accuracy when extrapolated to untested conditions (e.g., 450 °C and 550 °C), with flow stress prediction errors remaining below 8%. This level of predictive reliability confirms the model's robustness and generalisability, offering a powerful and time-efficient alternative to extensive experimental trials in the optimisation of thermomechanical processing parameters for biomedical titanium components.

A drawback of this model is its inability to describe the final phase of deformation—thermal softening. This is primarily because the model was originally developed for high-temperature viscoplastic deformation of metals where strain hardening and dynamic recovery dominate, but dynamic recrystallisation or flow softening mechanisms are not explicitly included.

One of the notable characteristics of the numerical results is the distinctive wavy shape of the stress-stress curve. This behaviour may be attributed either to the high deformation of some elements in the model, or numerical instability due too large time increments [38]. Wavy behaviour could also hint at a mismatch between strain-hardening and rate-dependence terms.

Postprocessing and output settings may also play a role. In simulations where stress is recorded at every increment, minor oscillations—often a natural part of the numerical solution—can become visually prominent. These fluctuations may not represent true physical behaviour but rather the discrete nature of the numerical integration. Smoothing techniques in postprocessing, or averaging over slightly larger strain intervals, can help distinguish between numerical noise and meaningful material response [39].

In summary, the wavy shape of the numerical stress–strain curves can be attributed to a combination of factors: time step sensitivity, material model parameter calibration, mesh resolution, and data sampling frequency. Addressing these issues through improved model tuning, mesh refinement, and careful solver control can enhance the fidelity of the numerical simulation as well as improve agreement with experimental observations.

Additionally, interpolation errors were observed at intermediate temperatures, especially at 500 °C, where the model's predictive accuracy decreased. This is due to the simplified approach of interpolating between parameters identified at 400 °C and 600 °C without additional calibration at the intermediate temperature. The model incorrectly assumes that the material behaviour at 500 °C closely follows the 400 °C trend, which results in an overestimation of flow stress. Incorporating more data points at finer temperature intervals or using temperature-dependent parameter functions could mitigate this issue in future studies.

Furthermore, the wavy shape of the simulated stress–strain curves (Figure 6) indicates the presence of numerical artefacts. These oscillations likely result from insufficient time step control, potentially combined with postprocessing settings that overemphasise incremental stress fluctuations. Mesh density and solver configuration may also contribute to this effect, particularly in the regions with large plastic deformation. Refining the time step strategy, improving mesh resolution, and applying smoothing techniques in postprocessing could reduce these artefacts and further improve the numerical stability and physical realism of the simulations [40].

Despite the model's strong overall performance, the discrepancies observed at lower temperatures

and in the softening phase suggest areas for improvement. Incorporating dynamic recrystallisation kinetics into the saturation stress term or coupling the Anand model with microstructure-sensitive approaches (e.g., crystal plasticity) could enhance accuracy. Deviations may also stem from experimental uncertainties, such as frictional variation or slight temperature gradients in the sample. More advanced calibration methods, including machine learning-assisted parameter optimisation, could further refine the model's predictive robustness under varied processing conditions [41].

The comparison between simulation and experimental results confirms that the Anand model provides a reliable and efficient tool for predicting the thermoplastic deformation of commercially pure titanium, particularly at elevated temperatures (400–600 °C) and moderate strain rates. The model accurately captures the overall shape and slope of the stress–strain curves in the plastic regime and demonstrates strong agreement across most tested conditions. The deviations observed at lower temperatures, especially at 400 °C, are likely due to dynamic recrystallisation, which is not explicitly modelled. At 500 °C, mismatches are attributed to the model's limited ability to capture transitional deformation mechanisms and possible interpolation errors between calibrated data points. Despite minor discrepancies, the model shows good predictive capability under untested conditions validating its application for process optimisation and implant design.

Future research should focus on enhancing the Anand model by incorporating mechanisms such as dynamic recrystallisation or coupling it with microstructure-sensitive models like crystal plasticity, especially to improve accuracy at lower and transitional temperatures [16, 42, 43]. Expanding the experimental dataset to include finer temperature intervals (e.g., every 25 °C) could improve parameter fitting and reduce interpolation errors. These developments would further increase the model's predictive precision and applicability in complex, multi-axial loading scenarios relevant to biomedical implant manufacturing.

Another important factor which cannot be neglected in future research is the matter of the uniformity of temperature. While the uniform temperature assumption is sufficient for model calibration and initial process optimisation, future work should address this limitation by incorporating thermal gradients into the simulation framework, possibly through coupled thermomechanical analysis. This would improve the model's applicability to industrial-scale processes where heat transfer, frictional heating, and temperature distribution across the part cannot be neglected.

Moreover, biomedical forming processes such as forging and extrusion involve complex, multiaxial stress states that can significantly affect material flow and microstructural evolution. Future work should also focus on extending the model validation to multiaxial deformation scenarios, including upsetting, torsion, or combined loading tests, to ensure the model's applicability to industrial-scale forming processes relevant to implant manufacturing. [44, 45].

This study demonstrated the successful adaptation of the Anand constitutive model for predicting the thermoplastic deformation behaviour of commercially pure titanium, addressing a key challenge in the optimisation of manufacturing processes for biocompatible orthopaedic implants. The model reliably captures the stress–strain response across a wide temperature range (400–600 °C), particularly excelling in the later stages of deformation where material flow is dominant. By eliminating the need for complex yield surface definitions, the model reduces experimental data requirements while retaining robust predictive capabilities. The calibrated material constants are consistent with the values reported in the literature, yet tailored to reflect the specific thermomechanical response of pure titanium.

Implementation in ANSYS enabled rapid, full-process simulations with computation times under 15 minutes per case, significantly accelerating parameter selection compared to traditional trial-and-error approaches. The model supports the design of implants with yield strengths up to 800 MPa, while preserving the intrinsic biocompatibility of titanium. Although discrepancies were observed at 400 °C, likely due to incomplete dynamic recrystallisation, these limitations can be addressed by incorporating recrystallisation kinetics into the saturation stress term or coupling the model with crystal plasticity approaches, particularly for sub-500 °C applications. Further validation under multiaxial loading, such as in forging or extrusion processes, is recommended.

The developed numerical framework enables detailed process planning and precise optimisation of deformation conditions, supporting the production of titanium implants with tailored mechanical properties and reliable performance in biomedical applications.

REFERENCES

1. Liang, S.: Review of the design of titanium alloys with low elastic modulus as implant materials. Adv. Eng. Mater. 2020; 22, 2000555. https://doi.org/10.1002/adem.202000555
2. Hussain, O., Saleem, S., Ahmad, B.: Implant materials for knee and hip joint replacement: A review from the tribological perspective. IOP Conf. Ser. Mater. Sci. Eng. 2019; 561, 012007. https://doi.org/10.1088/1757-899X/561/1/012007
3. Gheorghe, D., Pop, D., Ciocoiu, R., Trante, O., Milea, C., Mohan, A., Benea, H., Saceleanu, V.: Microstructure development in titanium and its alloys used for medical applications. 16.
4. Khadija, G., Saleem, A., Akhtar, Z., Naqvi, Z., Gull, M., Masood, M., Mukhtar, S., Batool, M., Saleem, N., Rasheed, T., Nizam, N., Ibrahim, A., Iqbal, F.: Short term exposure to titanium, aluminum and vanadium (Ti 6Al 4V) alloy powder drastically affects behavior and antioxidant metabolites in vital organs of male albino mice. Toxicol. Rep. 2018; 5, 765–770. https://doi.org/10.1016/j.toxrep.2018.06.006
5. Quinn, J., McFadden, R., Chan, C.-W., Carson, L.: Titanium for Orthopedic Applications: An Overview of Surface Modification to Improve Biocompatibility and Prevent Bacterial Biofilm Formation. iScience. 2020; 23, 101745. https://doi.org/10.1016/j.isci.2020.101745
6. Gomes, C.C., Moreira, L.M., Santos, V.J.S.V., Ramos, A.S., Lyon, J.P., Soares, C.P., Santos, F.V.: Assessment of the genetic risks of a metallic alloy used in medical implants. Genet. Mol. Biol. 2011; 34, 116–121. https://doi.org/10.1590/S1415-47572010005000118
7. Bańczerowski, J., Pawlikowski, M., Płociński, T., Zagórski, A., Sawicki, S., Gieleta, R.: New approach to $${\upalpha }$$-titanium mechanical properties enhancement by means of thermoplastic deformation in mid-temperature range. Contin. Mech. Thermodyn. 2024; 36, 1645–1660. https://doi.org/10.1007/s00161-024-01321-4
8. Bańczerowski, J., Pawlikowski, M.: New approach in constitutive modelling of commercially pure titanium thermo-mechanical processing. Contin. Mech. Thermodyn. 2021; 33, 2109–2121. https://doi.org/10.1007/s00161-021-01011-5
9. Dyja, H., Galkin, A.M., Knapiński, M.: Reologia metali odkształcanych plastycznie. Wydawnictwo Politechniki Częstochowskiej 2010.
10. Anand, L.: Constitutive equations for hot-working of metals. Int. J. Plast. 1985; 1, 213–231.
11. Chen, X., Chen, G., Sakane, M.: Prediction of stress-strain relationship with an improved Anand constitutive Model For lead-free solder Sn-3.5Ag. IEEE Trans. Compon. Packag. Technol. 2005; 28, 111–116. https://doi.org/10.1109/TCAPT.2004.843157
12. Cheng, Z.N., Wang, G.Z., Chen, L., Wilde, J., Becker, K.: Viscoplastic Anand model for solder alloys and its application. Solder. Surf. Mt. Technol. 2000; 12, 31–36. https://doi.org/10.1108/09540910010331428
13. Balasubramanian, S., Anand, L.: Elasto-viscoplastic constitutive equations for polycrystalline fcc materials at low homologous temperatures. J. Mech. Phys. Solids. 2002; 50, 101–126. https://doi.org/10.1016/S0022-5096(01)00022-9
14. Bai, N., Chen, X., Gao, H.: Simulation of uniaxial tensile properties for lead-free solders with modified Anand model. Mater. Des. 2009; 30, 122–128. https://doi.org/10.1016/j.matdes.2008.04.032
15. Anand, L., Narayan, S.: An Elastic-Viscoplastic Model for Lithium. J. Electrochem. Soc. 2019; 166, A1092–A1095. https://doi.org/10.1149/2.0861906jes
16. Puchi-Cabrera, E.S., Guérin, J.D., La Barbera-Sosa, J.G., Dubar, M., Dubar, L.: Plausible extension of Anand's model to metals exhibiting dynamic recrystallization and its experimental validation. Int. J. Plast. 2018; 108, 70–87. https://doi.org/10.1016/j.ijplas.2018.04.013
17. Zhang, Z., Chen, Z., Liu, S., Dong, F., Liang, K., Ma, K.: The comparison of Qian-Liu model and Anand model for uniaxial tensile test of SAC305. In: 2019 20th International Conference on Electronic Packaging Technology(ICEPT). 1–5. IEEE, Hong Kong, China 2019.
18. Zeng, Z., Zhang, Y., Jonsson, S.: Deformation behaviour of commercially pure titanium during simple hot compression. Mater. Des. 2009; 30, 3105–3111. https://doi.org/10.1016/j.matdes.2008.12.002
19. Sakai, T., Belyakov, A., Kaibyshev, R., Miura, H., Jonas, J.J.: Dynamic and post-dynamic recrystallization under hot, cold and severe plastic deformation conditions. Prog. Mater. Sci. 2014; 60, 130–207. https://doi.org/10.1016/j.pmatsci.2013.09.002
20. Zeng, Z., Jonsson, S., Roven, H.J.: The effects of deformation conditions on microstructure and texture of commercially pure Ti. Acta Mater. 2009; 57, 5822–5833. https://doi.org/10.1016/j.actamat.2009.08.016
21. Ahn, K., Huh, H., Yoon, J.: Rate-dependent hardening model for pure titanium considering the effect of deformation twinning. Int. J. Mech. Sci. 2015; 98, 80–92. https://doi.org/10.1016/j.ijmecsci.2015.04.008
22. Tan, M.J., Zhu, X.J.: Microstructure evolution of CP titanium during high temperature deformation. Arch. Mater. Sci. Eng. 2007; 28, 7.
23. Zhao, J., Ding, H., Zhao, W., Huang, M., Wei, D., Jiang, Z.: Modelling of the hot deformation behaviour of a titanium alloy using constitutive equations and artificial neural network. Comput. Mater. Sci. 2014; 92, 47–56. https://doi.org/10.1016/j.commatsci.2014.05.040

24. Hua, K., Zhang, Y., Tong, Y., Zhang, F., Kou, H., Li, X., Wang, H., Li, J.: Enhanced mechanical properties of a metastable β titanium alloy via optimized thermomechanical processing. Mater. Sci. Eng. A. 2022; 840, 142997. https://doi.org/10.1016/j.msea.2022.142997
25. Weiss, I., Semiatin, S.L.: Thermomechanical processing of alpha titanium alloys—an overview. Mater. Sci. Eng. A. 1999; 263, 243–256. https://doi.org/10.1016/S0921-5093(98)01155-1
26. Zhang, L., Pellegrino, A., Townsend, D., Petrinic, N.: Thermomechanical constitutive behaviour of a near α titanium alloy over a wide range of strain rates: Experiments and modelling. Int. J. Mech. Sci. 2021; 189, 105970. https://doi.org/10.1016/j.ijmecsci.2020.105970
27. Bańczerowski, J., Jeleńkowski, J., Skalski, K., Sawicki, S., Wachowski, M.: Structure and mechanism of the deformation of Grade 2 titanium in plastometric studies. Mater. Sci. Technol. 2019; 35, 253–259. https://doi.org/10.1080/02670836.2018.1443608
28. Chen, G., Zhang, Z.-S., Mei, Y.-H., Li, X., Yu, D.-J., Wang, L., Chen, X.: Applying viscoplastic constitutive models to predict ratcheting behavior of sintered nanosilver lap-shear joint. Mech. Mater. 2014; 72, 61–71. https://doi.org/10.1016/j.mechmat.2014.02.001
29. Titanium Alloy Guide, https://www.spacematdb.com/spacemat/manudatasheets/TITANIUM%20ALLOY%20GUIDE.pdf., 2000.
30. Bańczerowski, J.: Proces technologiczny oraz modelowanie numeryczne obróbki termoplastycznej tytanu na potrzeby inżynierii biomedycznej: rozprawa doktorska, 2023.
31. Banerjee, S., Mukhopadhyay, P.: Phase Transformations: Examples from Titanium and Zirconium Alloys. Elsevier, 2010.
32. Franklin, S.V., Mertens, F., Marder, M.: Portevin-Le Chatelier effect. Phys. Rev. E. 2000; 62, 8195–8206. https://doi.org/10.1103/PhysRevE.62.8195
33. Prasad, K., Varma, Vijay.K.: Serrated flow behavior in a near alpha titanium alloy IMI 834. Mater. Sci. Eng. A. 2008; 486, 158–166. https://doi.org/10.1016/j.msea.2007.09.020
34. Nemat-Nasser, S., Guo, W.G., Cheng, J.Y.: Mechanical properties and deformation mechanisms of a commercially pure titanium. Acta Mater. 1999; 47, 3705–3720. https://doi.org/10.1016/S1359-6454(99)00203-7
35. Levie, R. de: Curve Fitting with Least Squares. Crit. Rev. Anal. Chem. 2000. https://doi.org/10.1080/10408340091164180
36. Motulsky, H.J., Ransnas, L.A.: Fitting curves to data using nonlinear regression: a practical and nonmathematical review. FASEB J. 1987; 1, 365–374. https://doi.org/10.1096/fasebj.1.5.3315805
37. Arlinghaus, S.: Practical Handbook of Curve Fitting. CRC Press, Boca Raton, 2023.
38. Ardourel, V., Jebeile, J.: Numerical instability and dynamical systems. Eur. J. Philos. Sci. 2021; 11, 49. https://doi.org/10.1007/s13194-021-00372-7
39. Franz, S.: Post-processing and improved error estimates of numerical methods for evolutionary systems. IMA J. Numer. Anal. 2024; 44, 2936–2958. https://doi.org/10.1093/imanum/drad082
40. Rice, J.R.: Numerical Methods in Software and Analysis. Elsevier, 2014.
41. Anand, L.: Elasto-viscoplasticity: Constitutive modeling and deformation processing. In: Large Plastic Deformations: Fundamental Aspects and Applications to Metal Forming. Routledge, 1993.
42. Abdolvand, H.: Development of microstructure-sensitive damage models for zirconium polycrystals. Int. J. Plast. 2022; 149, 103156. https://doi.org/10.1016/j.ijplas.2021.103156
43. Tran, A., Wildey, T., Lim, H.: Microstructure-sensitive uncertainty quantification for crystal plasticity finite element constitutive models using stochastic collocation methods. Front. Mater. 2022; 9. https://doi.org/10.3389/fmats.2022.915254
44. Geetha, M., Singh, A.K., Asokamani, R., Gogia, A.K.: Ti based biomaterials, the ultimate choice for orthopaedic implants – A review. Prog. Mater. Sci. 2009; 54, 397–425. https://doi.org/10.1016/j.pmatsci.2008.06.004
45. Zhang, L., Chen, L.: A Review on Biomedical Titanium Alloys: Recent Progress and Prospect. Adv. Eng. Mater. 2019; 21, 1801215. https://doi.org/10.1002/adem.201801215